17th World Conference on Earthquake Engineering, 17WCEE

Sendai, Japan - September 13th to 18th 2020

Seismic Repair by Retightening Turnbuckle Brace

S. Nakada[(1)], S. Kishiki[(2)]

[(1)] *Doctoral student, Tokyo Institute of Technology, nakada.s.ag@m.titech.ac.jp*
[(2)] *Associate professor, kishiki.s.aa@m.titech.ac.jp*

Abstract

This paper focuses on the performance recovery of braces by retightening the turnbuckle. In order to investigate performance recovery, workability, and additional inter forces when the turnbuckle is retightened, loading tests were conducted. The findings obtained from the tests are summarized as follows: (1) The performance recovery of brace is not affected by multiple retightening of the turnbuckle and, the workability of repair does not decrease. (2) The additional inter forces can be grasped by using the dynamic model proposed in this paper.

Keywords: Seismic repair, Turnbuckle brace, Performance recovery, Workability, Additional inter forces,

1. Introduction

In Japan, gymnasiums are often used as evacuation facilities during disasters. However, Japanese seismic design places the highest priority on the protection of human life and allows damage to buildings. As a result, many gymnasiums are damaged, and evacuation facilities were not enough [1]. Therefore, it is necessary to establish a seismic repair that can make the building being used continuously after an earthquake event, although the damage reduction is also important.

The authors have studied methods for quantitatively evaluating damage based on the damage degree [2-4]. In this paper, as a part of these studies, the performance recovery by retightening the turnbuckle brace and the additional inter force due to brace deformation are clarified by structural experiments.

2. Experimental plan

2.1 Specimens

The outline and specifications of the specimens are shown in Fig.1 and Table.1. Specimens are a turnbuckle brace composed of battledore plates, a round bar, and a turnbuckle. Referring to “Design and Construction Recommendation for Turnbuckle for building” [5] in Japan, the specimens were designed to be full-size tensile braces used in standard gymnasium. The experiment parameters are the nominal size, connection eccentricity, and the length of the gusset plate (G.PL). The performance recovery and workability differences by retightening the turnbuckle brace are confirmed by the parameters. In addition, the additional inter forces will be investigated by using the specimens with the various thickness of G.PL.

2.2 Setup

The setup and the measuring equipment are shown in Fig.2(a). The end of specimens is attached to the reaction jig and the other end is fixed on the oil jack via the sliding jig. The experiment was conducted by giving a displacement in the axial direction using the oil jack.

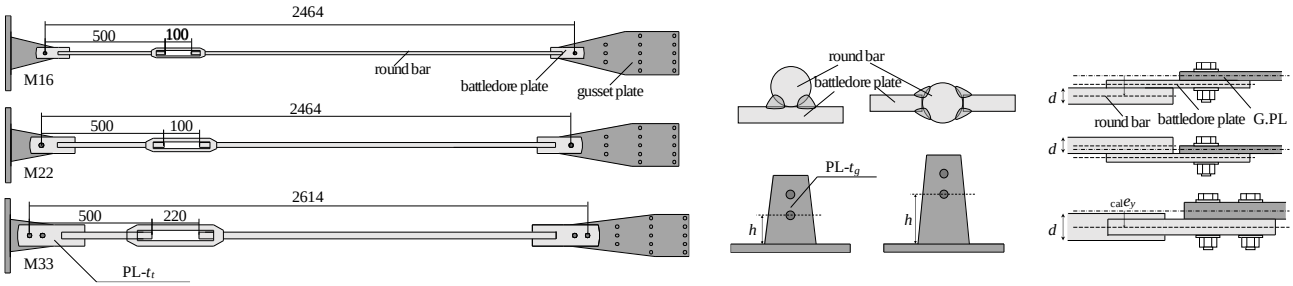

Fig.1- Outline of specimens

Table.1- Specifications of specimens

Specimen	Nominal size	d [mm]	L [mm]	t_h [mm]	h [mm]	t_q [mm]	$_{cal}e_y$ [mm]
A	M16	14.5	2464	6	160	6	-5.0
B							17.0
C						9	18.5
D						12	20.0
E						25	26.5
F	M22	20.0		9	145	9	-6.5
G							24.5
H	M33	30.3	2614	12		12	12.5
I					85		

2.3 Measurement plan

2.3.1 Measurement of brace behaviors

The axial deformation of the brace (δ) was calculated from the absolute displacements (d_1, d_2) from the end plate of the specimen and the relative displacement (d_3) from the reaction force jig. The axial force (N_x) was measured by a 300kN loadcell attached to the reaction jig. Tensile is positive and compression is negative for the axial force and axial deformation.

2.3.2 Measurement of torque

In this paper, torque (T) was used as an index of workability in order to understand how much force is required for retightening the turnbuckle brace. The measuring equipment for torque is shown in Fig.2(b). The fixing jig was attached to the turnbuckle part of the test specimen. The turnbuckle was retightened via a measuring jig, coupler, and PC steel bar. The torque (T) was measured by two strain gauges attached to the top and bottom of the measuring jig. Furthermore, the torque coefficient (k_T) is obtained from the following equation.

$$k_T = \frac{T}{d \cdot N_x} \tag{1}$$

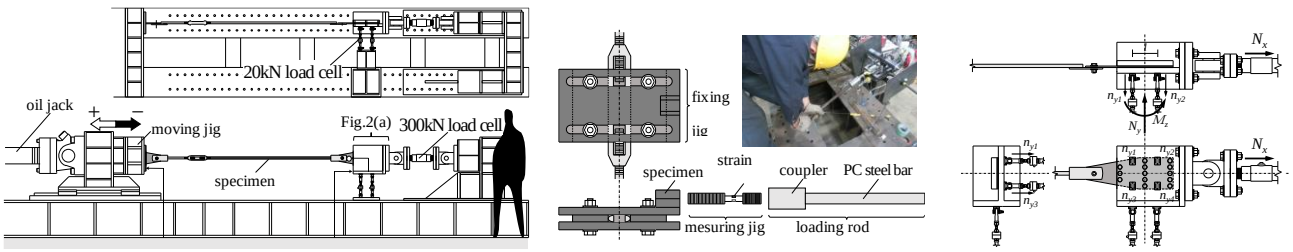

(a)- Setup (b)-Mesurement of torque (c)- Mesurement of additional inter forces

Fig.2- Measurement plan

2.3.3 Measurement of additional inter forces

In this study, the out-of-plane bending moment (M_z) is considered as additional inter forces. The out-of-plane bending moment was calculated by the 20kN load cell connected to the reaction jig (Fig.2(c)). The additional inter force is transmitted to the pin member incorporating the 20kN load cell. The out-of-plane bending moment (M_z) can be calculated by the following equation if the additional inter force acting on the pin member is n_{y1}, n_{y2}, n_{y3}, n_{y4}.

$$M_z = (n_{y1} + n_{y3} - n_{y2} - n_{y4}) \cdot \frac{l}{2} \tag{2}$$

The out-of-plane bending moment is positive clockwise, and the eccentric distance is positive in the direction that the battledore plates are attached from the G.PL. Also, in all the specimens, the battledore plates were attached in the direction of the 20kN loadcell.

2.4 Loading protocol

The outline of the loading protocol is shown in Fig.3. The vertical axis is the average strain (ε) obtained by dividing the axial deformation (δ) by the length of the specimen (L), and the horizontal axis is the number of steps. The basic loading history is a reversed cyclic loading with the amplitudes of ε = 0.125, 0.25, 0.50, 0.75, 1.00, 1.50, 2.00% repeated for two cycles each. One set of loading consists of three cycles as shown in Fig.3. The first two cycles which have different amplitudes are called “damage loading”. After performing the damage loading, the deformation is returned to zero, and the seismic repair is conducted by retightening the turnbuckle brace. After that, the last cycle of the set which has the same amplitude as the previous cycle is performed; this last cycle is called “after repair loading”. As shown in Fig.3, the second cycle of each amplitude is considered as the after repair loading in the current set and as the damage loading in the following set. The performance recovery is confirmed by comparing the performance under the damage loading and after repair loading within one set.

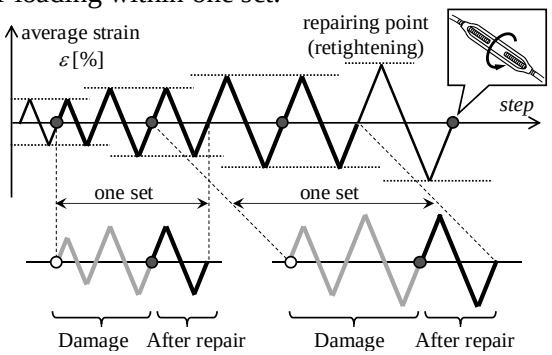

Fig.3- Outline of loading protocol

3. Test result

3.1 Axial force – average strain relationship

The hysteresis behaviors obtained from the experiment are shown in Fig.4. The vertical axis is the axial force (N_x), and the horizontal axis is the average strain (ε). The figure shows the average strain for each amplitude, and the type of line distinguished the type of load.

It can be seen from the figure that the hysteresis curve under “after repair loading” is greater than that of under “damage loading” which indicates that the performance of the brace has been restored by retightening the turnbuckle brace. Moreover, the maximum strength of “damage loading” and the yield strength of “after repair loading” is almost equal, and the secondary stiffness is almost the same. In other words, it can be said that the relationship between the axial force and the average strain is a continuous hysteresis curves regardless of whether the turnbuckle brace is retightened or not.

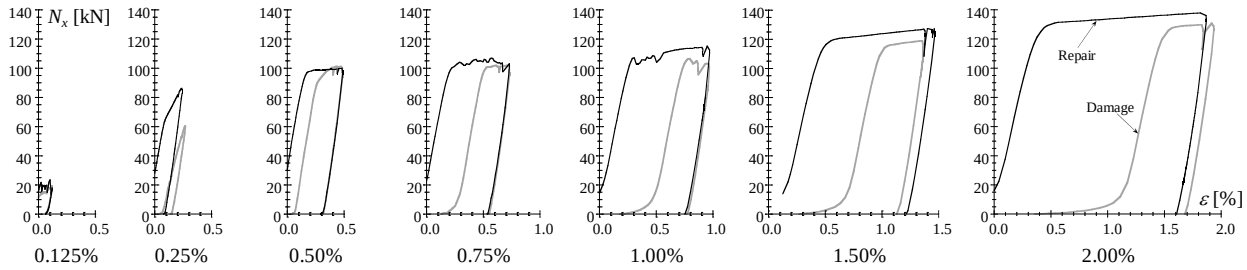

Fig.4- Axial force – average strain relationship

3.2 Axial force – cumulative average strain relationship

The relationship between the axial force (N_x) and the cumulative average strain ($\Sigma\varepsilon$) is shown in Fig.5. The line type distinguishes the difference in the joint of the brace, i.e., the eccentric distance, the thickness of G.PL (t_g), and the length of G.PL. However, it can be seen that regardless of the difference in the brace joints, almost the same curve is obtained for the specimens with the same nominal size. Therefore, it can be said that the difference in brace joints do not affect the performance recovery by retightening turnbuckle brace.

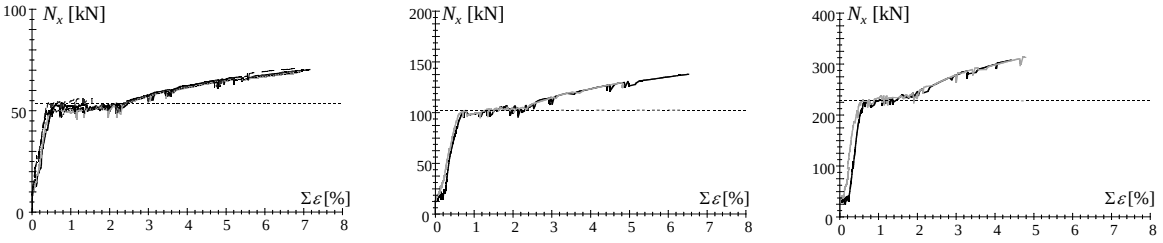

(a)M16 (b)M22 (c)M33

Fig.5- Axial force – cumulative average strain relationship

4. Performance recovery

In this section, the performance recovery by multiple repairs is evaluated. The relationship between performance recovery and the cumulative average strain ($\Sigma\varepsilon$) is shown in Fig.6. Maximum strength (Fig.6(a)), yield strength (Fig.6(b)), and elastic stiffness (Fig.6(c)) are focused as the performance recovery. The vertical axis for Fig.6(a), (b), and (c) are the ratio of the elastic stiffness after repair to Young's modulus E of steel, the ratio of the maximum strength in damage to that of after repair, and the yield strength in damage to that of after repair, respectively. Meanwhile, the horizontal axis in all figures is the cumulative average strain.

The ratio of elastic stiffness decreases as the cumulative strain increases, and the ratio in all cases is less than 1.0 which is identified to occur because of the local bending yield caused by the connection eccentricity between the round bar and the battledore plate as found by Kyuuko et al [6]. Moreover, the yield strength and maximum strength, ${}_rQ_{max}/{}_dQ_{max}$ (Fig.6(b)) and ${}_rQ_y/{}_dQ_y$ (Fig.6(c)), are larger than 1.0 in almost all cases which indicated that the performance recovery of brace is not affected by multiple retightening of the turnbuckle.

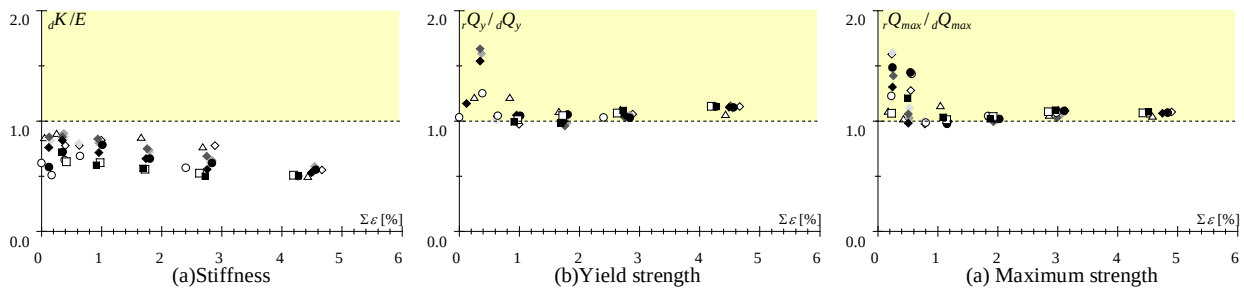

(a)Stiffness (b)Yield strength (a) Maximum strength

Fig.6- Performance recovery by retightening turnbuckle

5. Workability

5.1 Hysteresis behavior of turnbuckle brace under retightening

The hysteresis behavior when the retightening is conducted is shown in Fig.7. The horizontal axis is the number of steps, and the vertical axes are the torque (T), the axial force (N_x), and the rotation angle of GPL (θ_j). At the beginning of the retightening, the values of the axial force and the torque are relatively small, but they increase sharply at a certain point. Furthermore, looking at the angle of G.PL, the values of the axial force and the torque sharply increase at θ_j =0.0. Therefore, "restored" point can be defined when θ_j =0.0. In other words, the torque is relatively small due to no axial force until the angle of GPL is restored. Moreover, it can be seen that after the repair of G.PL, the torque increases together with the axial force.

5.2 Torque coefficient of multiple retightening turnbuckle brace

The relationship between the torque coefficient (k_T) and the cumulative average strain ($\Sigma\varepsilon$) is shown in Fig.8. The vertical axis is the torque coefficient (k_T), and the horizontal axis is the cumulative strain ($\Sigma\varepsilon$). The marker in figure distinguishes the nominal size. It can be seen that the torque coefficient is stable although the cumulative average strain increased. This means that the turnbuckle is not damaged even after many repairs, and the effect of retightening was exerted.

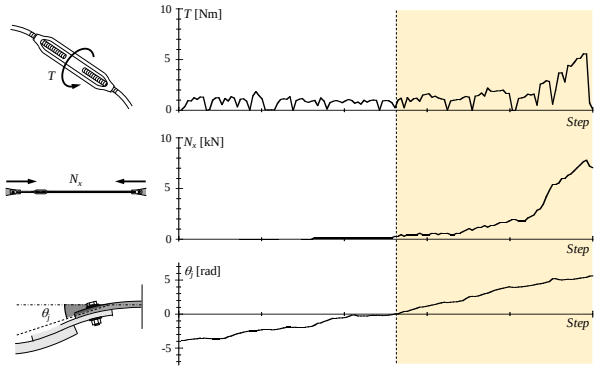

Fig.7- Hysteresis behavior under retightening

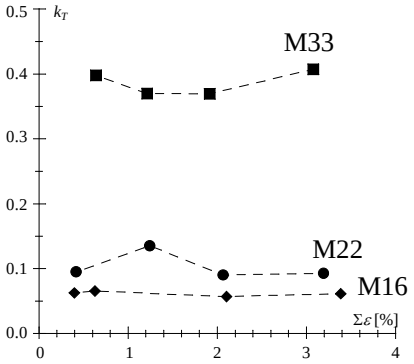

Fig.8- Workability of multiple repair

6. Additional inter forces

6.1 Hysteretic Behavior of additional inter forces

The hysteretic behavior of the axial force (N_x) and the out-of-plane bending moment (M_z) obtained by the experiment is shown in Fig.9. The vertical axis represents the axial force (N_x) and the out-of-plane bending moment (M_z), and the horizontal axis represents the average axial strain (ε). Here, the result of specimen C with ε =1.00% is shown.

In tension, the axial force (N_x) and the out-of-plane bending moment (M_z) are stable near ε = 0.25%, and both histories are similar. Meanwhile, in compression, the axial force (N_x) is almost zero in at ε = 1.20% due to overall buckling, while the out-of-plane bending moment (M_z) tended to increase sharply.

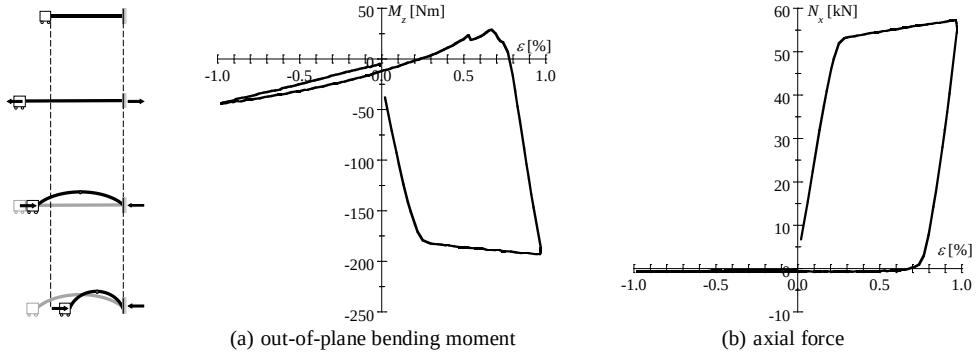

(a) out-of-plane bending moment (b) axial force

Fig.9- Hysteresis behavior of axial force and out-of-plane bending moment

6.2 Additional inter forces in tension

In this section, the evaluation method of the out-of-plane bending moment in tension is examined. First, the connection eccentricity of the brace is considered. The vertical eccentric distance (e_y) can be obtained from the following equation by using the relationship between the out-of-plane bending moment ${}_{exp}M_z$ and the axial force ${}_{exp}N_x$ (Fig.10(a)).

$$e_y = {}_{exp}M_z \,/\, {}_{exp}N_x \tag{3}$$

If the line of action of G.PL and the battledore plate are the same, the apparent connection eccentricity will be zero. However, the eccentric bending moment is zero because the eccentric distance between the battledore plate and the round bar and between the battledore plate and the G.PL is different. Therefore, the eccentric distance (${}_Te_y$) assumed in tension is expressed by the following equation.

$$ {}_Te_y = \frac{d - t_g}{2} \tag{4}$$

The eccentric distance in the experiment and the design is shown in Fig.10(b). The vertical axis is the eccentric distance (e_y), and the horizontal axis represents specimens. The markers in the figure distinguish the kind of eccentric distance. ● is the eccentric distance in the experiment (${}_{exp}e_y$), △ and □ are the eccentric distance in design (${}_{cal}e_y$). The distance between the center of the G.PL and the round bar is indicated as △, and the distance obtained by equation (4) is indicated as □.

In the case of specimen A and F with small eccentric distances due to the joining method, the eccentric distance in the experiment (●) corresponds well with the eccentric distance (□) in the design. On the other hand, looking at specimens B, C, D, and E with large eccentric distances due to the joining method, the experimental eccentric distance (●) does not correspond to the eccentric distance (□) at the time of design. From the above finding, the eccentric distance (□) in design can not be used as the eccentric distance for estimating the out-of-plane bending moment.

The eccentric distance obtained by equation (4) (△) is focused. It can be seen that the eccentric distance (△) corresponds well with the eccentric distance in the experiment (●). From this, it can be said that the eccentric distance in tension can be estimated by equation (4). In other words, from equation (4), it is thought that the out-of-plane bending moment in tension can be suppressed by making the thickness of G.PL equal to the diameter of the round bar.

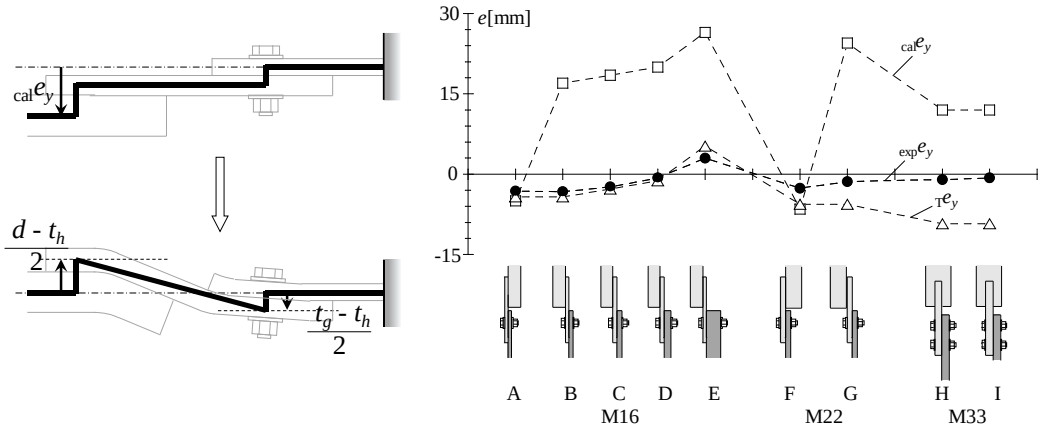

(a) Model in tension of brace (b) Stiffness

Fig.10- Vertical eccentric distance

6.3 Additional inter forces in compression

Here, the method of estimating the out-of-plane bending moment in compression is discussed. The model in compression is a cantilever from end of the G.PL to the inflection point, and the out-of-plane bending moment (M_z) in compression is calculated from the axial force (N_x) acting on the inflection point.

The method of calculating the inflection point is shown in Fig.11(a). The model of the entire brace is a compression member with rotational spring stiffness at both ends. Rotational spring stiffness (K_r) is expressed by the following equation [7].

$$K_r = \frac{\alpha \sin\alpha}{\cos\alpha - 1} \cdot \frac{EI}{L} \qquad \left(\alpha = \sqrt{\frac{{}_{\exp}N_{cr} L^2}{EI}} \right) \tag{5}$$

The deformation ($u_c(x)$) at the center of the brace, the rotation angle (θ_0) at the end of the brace, and the out-of-plane deformation ($y(x)$) of the brace for any x can be expressed by the following equations [7].

$$u_c(x) = \sqrt{\frac{5}{12} \cdot \frac{(k_r+8)^2}{({k_r}^2+14k_r+64)}} \cdot \sqrt{L \cdot x} \qquad \left(k_r = \frac{K_r L}{EI} \right) \tag{6}$$

$$\theta_0(u_c) = \frac{24}{L(k_r+8)} u_c(x) \tag{7}$$

$$y(x) = \left\{ -\frac{4}{3L^2}\left(\frac{k_r}{2}+1\right)x^3 + \frac{k_r}{2L}x^2 + x \right\} \theta_0(u_c) \tag{8}$$

The curvature ($M(x)/EI$) is obtained by performing second-order differentiation of equation (8). Since the inflection point is $M(x)/EI = 0$, the inflection point x_0 is expressed by the following equation.

$$x_0 = \frac{K_r L^2}{4K_r L + 8EI} \tag{9}$$

Further, the out-of-plane displacement y_0 at the inflection point is obtained by substituting equation (9) into equation (8). The out-of-plane bending moment M_z in compression can be estimated by the following equation.

$${}_{\text{cal}}M_z = N_x \cdot (y_0 + {}_{\text{cal}}e_y) + N_x \tan\theta_0 \cdot x_0 \tag{10}$$

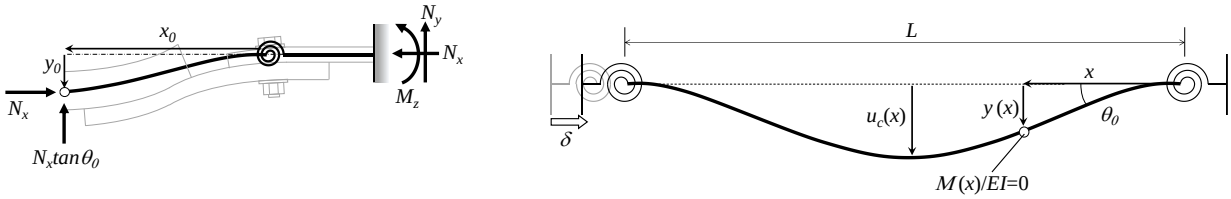

(a) Model of brace

(b)Calculation of inflection point

Fig.11- Out-of-plane bending moment in compression

6.4 Validation of the proposed model and equations

To validate the analytical model, the analytical and experimental values are compared. The analysis results are shown in Fig.12. The expression in the figure is the same as Fig.9, the experimental value is represented by the solid line, and the analytical value is represented by the broken line. The initial stiffness of the analysis model was E = 205000 [N/ mm^2], the yield strength was obtained from the mill test report, and the secondary stiffness is estimated to be about 2% of the initial stiffness.

Although the calculated out-of-plane bending moment ($_{cal}M_z$) is overestimated by about 75 [kN], the models in Fig.11 can be said to be effective because the history of the experimental values is almost the same as the analytical one. In other words, by using equation (10), it can be said that the out-of-plane bending moment in compression can be evaluated conservatively.

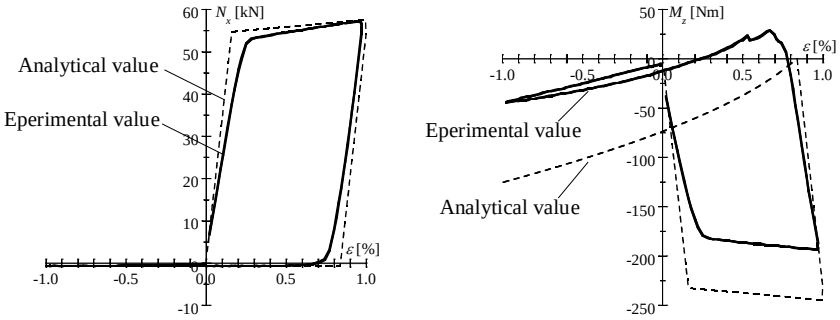

(a) axial force (b) out-of-plane bending moment

Fig.12- Experimental value and analytical value

7. Conclusion

This paper focused on the performance recovery by retightening the turnbuckle brace and the additional inter force due to brace deformation. The results obtained are shown below.

(1) Despite the differences in joints, damaged braces recover their performance by retightening the turnbuckles. In addition, the number of repairs did not affect the performance recovery of the maximum strength and yield strength, but it affected the elastic stiffness by decreasing it.

(2) Workability by retightening the turnbuckle is stable even if it was performed multiple times.

(3) The connection eccentricity of the turnbuckle brace in tension can be obtained by using the equation proposed in this paper.

(4) The model of the out-of-plane bending moment of the brace in compression is proposed in the paper, and its effectiveness was confirmed by comparing it with the experimental results.

8. Acknowledgements

This work was supported by JST Program on Open Innovation Platform with Enterprises, Research Institute Academia, Grant -in-Aid for Scientific Research (B).

9. References

[1] Iyama J, Yamada S, Matsumoto Y, Kishiki S, Koyama T, Shimada Y (2013): Seismic damage to vertical braces in steel school buildings due to the 2011 TOHOKU earthquake, *Earthquake Engineering & Structural Dynamics*, **31** (3), p.p491-514 (in Japanese)

[2] Kishiki S, Yamada S (2014): Damage evaluation based on crack pattern and its width on the concrete foundation of exposed column base, *J. Struct. Constr. Eng. AIJ, Vol.*79 *No.*704, p.p1547-1557 (in Japanese).

[3] Kishiki S, Tatsumi N (2016): Damage evaluation based on the residual out-of-plane deformation and the leg opening of single angle brace, *J. Struct. Constr. Eng. AIJ, Vol.*81 *No.*719, p.p143-153, (in Japanese)

[4] Kishiki S, Iwasaki Y (2017): Evaluation of residual strength based on local buckling deformation of steel column, *J. Struct. Constr. Eng. AIJ, Vol.*82 *No.*735, p.p735-743 (in Japanese)

[5] Japanese Society of Steel Construction (2005): Design and Construction Recommendation for Turnbuckle for building, 3rd edition (in Japanese).

[6] Kyuuko H, Hirano M, Hodzumi H (1984): Test on initial stress control of turnbuckle brace, *Summaries of Technical Papers of Annual Meeting Architectural Institute of Japan, Vol.*59, p.p1559-1560 (in Japanese)

[7] Inoue K, Suita K (2017): Kenchikukoukouzou-sonorirontosekkei-, 3rd edition, p.p3.13-3.14 (in Japanese)

